Abdalla *et al. EURASIP Journal on Advances in Signal Processing* (2016) 2016:104
DOI 10.1186/s13634-016-0403-6

EURASIP Journal on Advances in Signal Processing

RESEARCH Open Access

Subarray-based FDA radar to counteract deceptive ECM signals

Ahmed Abdalla*, Wen-Qin Wang, Zhao Yuan, Suhad Mohamed and Tang Bin

Abstract

In recent years, the frequency diverse array (FDA) radar concept has attracted extensive attention, as it may benefit from a small frequency increment, compared to the carrier frequency across the array elements and thereby achieve an array factor that is a function of the angle, the time, and the range which is superior to the conventional phase array radar (PAR). However, limited effort on the subject of FDA in electronic countermeasure scenarios, especially in the presence of mainbeam deceptive jamming, has been published. Basic FDA is not desirable for anti-jamming applications, due to the range-angle coupling response of targets. In this paper, a novel method based on subarrayed FDA signal processing is proposed to counteract deceptive ECM signals. We divide the FDA array into multiple subarrays, each of which employs a distinct frequency increment. As a result, in the subarray-based FDA, the desired target can be distinguished at subarray level in joint range-angle-Doppler domain by utilizing the fact that the jammer generates false targets with the same ranges to each subarray without reparations. The performance assessment shows that the proposed solution is effective for deceptive ECM targets suppression. The effectiveness is verified by simulation results.

Keywords: Frequency diverse array (FDA) radar; Electronic counter countermeasure (ECCM); Deceptive jamming; Subarray level

1 Introduction

Multifunction phased-array radar (PAR) is a specialized application of general PAR technology, designed to simultaneously fulfill the multiple functions of national air and weather surveillance [1, 2]. Due to its ability to form and steer the radar beam electronically, and to reconfigure the beam between any two transmitted pulses or even between transmit and receive modes, PAR permits multiple functions to be carried out with the same radar.

Therefore, PAR has been frequently used in the military for aircraft surveillance and tracking. However, with the application of military radar, the electronic countermeasures (ECM) have undergone intensive development, resulting in a considerable challenge to the PAR and airborne early warning (AEW) radars. Basically, space-time adaptive processing (STAP) is an essential technique to detect slowly moving targets in strong clutter background [3–6].

*Correspondence: ahmed.baoney6@hotmail.com
School of Electronic Engineering, University of Electronic Science and Technology of China, 610054 Chengdu, China

Necessities of current radar systems are becoming even more demanding in modern electronic warfare ECM scenarios, especially in existence of deceptive jamming because of its high efficiency. Deceptive ECM, an efficient division of ECM techniques, mainly creates deceptive targets to fail to take advantage of the useful information or saturate the target extraction and tracking algorithms, which leads to confusion on detecting and determining the true target. More particularly, in the case that the jammer has been carried by the target, the same range ratio between the target and the jammer will be obtained.

Consequently, with the advancement of digital radio frequency memory (DRFM) [7, 8], the active false targets retransmitted by deception jammers would be robustly correlated with real target echoes and probably overlap with the echoes in both time and frequency domain, which will significantly enhance its deception. More precisely, the active false targets generate a coherent pulse train of the same carrier frequency, modulation type, pulse width, and pulse repetition frequency (PRF). Therefore, the randomization of the scan-to-scan range delay of the jammer pulse, and adjustable linear initial phase

advancement over the pulse train will be achieved. In effect, contrary to unintentional contaminating targets that are ordinarily not very powerful, active ECM perfectly created false targets with random range and Doppler. In view of that, false targets with scan-to-scan randomized range and Doppler clearly become a potentially dangerous threat. Therefore, more awareness should be driven to their potential abilities in the electronic counter-countermeasure (ECCM), which is of vital prominence to the survival and operation performance of radar systems in electronic warfare.

Extensive studies have been done on the ECCM to combat deceptive jamming, such as pulse diversity [9–11], motion features discrimination [12], and data fusion-based methods [13–15]. Nevertheless, they are not accessible for FDA, since the ECCM ability is limited into a one-dimensional view and current FDA research concentrates mainly on analyzing the range-dependent beam pattern characteristics. Thus, further investigations should be carried out to develop FDA ECCM methods.

More recently, an FDA acting as the transmit array to mitigate the clutter, suppressive and deceptive jamming in a multiple-input multiple-output (MIMO) STAP radar is proposed in [16]. The cancelation was based on combining the range, angle, and Doppler domains in FDA-MIMO-STAP radar. In [17], the FDA-MIMO radar to suppress the deceptive jamming in joint transmit-receive domain has been investigated. The suppression was based on the fact that FDA-MIMO radar steering vector is dependent on both range and angle. Therefore, the false targets can be suppressed due to the mismatch in either range or angle. This method works well only when the angle of the false target is different from that of the true target, or when they are in close angle but far from each other in the range. However, the discrimination performance will deteriorate severely when the ranges of the false and true target are too close. Although the MIMO radar has a number of advantages, it suffers from a significant disadvantage, that is, the absence of the coherent joint transmit/receive processing gain [18].

In PAR system, subarray technique, which is an effective way to reduce the dimension and to realize the partially adaptive STAP, is usually adopted in STAP application. A creative and pioneering contribution to the PAR subarray aspects includes subarrayed weighting for side loop canceler, subarrayed adaptation and super resolution, and subarray optimization, which have been investigated in [19]. In [20–22], transmitted subaperturing schemes for range and angle estimation in FDA radar have been addressed. Predominantly, the studies on PAR and FDA radar mostly concentrate on clutter suppression, rarely focusing on deception jamming suppression, and fundamentally at the elementary level.

The main contribution of this paper is to provide the FDA subarray level for countering the deception jamming, according to the fact that the DRFM repeated jammer can hardly create false targets with appropriated range related for each element/subarray due to frequency offsets. In doing so, the true target's range and angle can be estimated correctly from the different amplitude responses of the subarrays in the target position and these are the preconditions for false targets suppression. Thus, even in situations where the false and true target are too close, the deceptive jamming suppression can be handled with the subarray-based FDA radar.

The rest of the paper is organized as follows. In Section 2, an introduction to FDA characteristics is given. In Section 3, we present the subarray-based FDA radar signal model for false targets suppression. Then, in Section 4, the simulation results are provided to confirm the effectiveness of the proposed method. Finally, conclusions are drawn in Section 5.

2 Background and Motivation

FDA, due to its unique range-angle-dependent beampattern, in contrast to angle-dependent beam pattern of PAR, is nowadays a quite well recognized theory and many interesting papers are published. The pioneering works of Antonik and Wicks et al. [23–26] opened the access of this demanding research field. Since then, numerous ideas based on different design criteria and assumptions for the array structure, have been proposed and evaluated.

The most important difference of the FDA, in conflict to PAR, is that there is a small frequency increment in the carrier frequency used across the elements and therefore making the array beam focusing direction vary as a function of the range, angle, and time.

For simplicity and without loss of generality, let us consider a uniform linear FDA (ULA) which radiates at each array element identical waveform signal, but with a frequency increment Δf Hz as shown in Fig. 1. Thus, the frequency radiated from the nth FDA elements can be represented by [20–22]

$$f_n = f_0 + n\Delta f \qquad \text{and} \qquad n = 0, 1, 2, \ldots, N-1, \quad (1)$$

where f_0 denotes the FDA carrier frequency, λ is the wavelength, and N is the number of the antenna elements.

The phase shift due to the path length in FDA is denoted by

$$\psi = \frac{2\pi}{\lambda} d \cos\theta, \quad (2)$$

where the angle θ defines the direction of the target from the axis of the array.

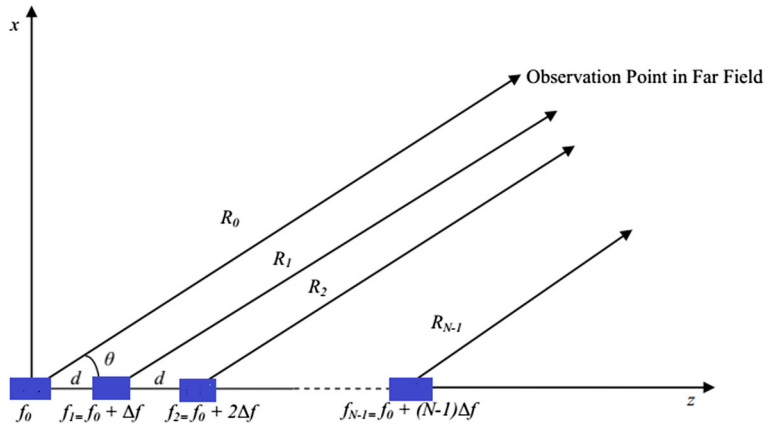

Fig. 1 ULA FDA with frequency increment Δf

The phase of the signal arriving at the first element f_0, which is taken as reference can be recast as

$$\psi = \frac{2\pi}{\lambda} R_0 = \frac{2\pi f_0}{c} R_0, \tag{3}$$

where f_0 is the frequency of the waveform emitted from first element, c is the speed of light and is the path length between the element, and R_0 is the far-field observation point. Likewise, the phase of the signal arriving at element one can be written as

$$\begin{aligned} \psi_1 &= \frac{2\pi f_1}{c} R_1 = \frac{2\pi (f_0 + \Delta f)}{c} (R_0 - d\cos\theta) \\ \psi_1 &= \frac{2\pi f_0 R_0}{c} + \frac{2\pi(\Delta f) R_0}{c} - \frac{2\pi f_0 d\cos\theta}{c} \\ &\quad - \frac{2\pi(\Delta f) d\cos\theta}{c}. \end{aligned} \tag{4}$$

Note that the approximation $R_{N-1} \approx R_0 - (N-1)d\cos\theta$ is adopted in Eq. (4).

The phase difference between the signals arriving at the first element and the second element can be expressed by

$$\begin{aligned} \psi_0 - \psi_1 &= \frac{2\pi f_0}{c} R_0 - \left(\frac{2\pi f_0 R_0}{c} + \frac{2\pi(\Delta f) R_0}{c} \right. \\ &\quad \left. - \frac{2\pi f_0 d\cos\theta}{c} - \frac{2\pi(\Delta f) d\cos\theta}{c} \right) \\ \Delta\psi &= \frac{2\pi f_0 d\cos\theta}{c} + \frac{2\pi(\Delta f) d\cos\theta}{c} - \frac{2\pi(\Delta f) R_0}{c}. \end{aligned} \tag{5}$$

Equation 5 can be interpreted by the fact that the first term is basically the conventional array factor seen regularly in array theory if we use $\frac{f_0}{c} = \frac{1}{\lambda}$. The second term is small and can be ignored [20]. The last term is very important, since it shows that the array radiation pattern depends on the range and the frequency increment.

The last terms in Eq. (5) create an apparent angle contradictory to the scan angle that one usually sees in PAR. This apparent scan angle can be derived using the same considerations in PAR. Thus, due to the change in the angle, progressive phase shift must be defined in terms of the apparent angle as follows

$$\Delta\psi = \frac{2\pi}{\lambda} d\cos\theta_a, \tag{6}$$

where θ_a is the apparent angle. Equating Eq. (6) to Eq. (5) results in

$$\begin{aligned} \Delta\psi &= \frac{2\pi f}{c} d\cos\theta_a \\ &= \frac{2\pi f_0 d\cos\theta}{c} + \frac{2\pi(\Delta f) d\cos\theta}{c} - \frac{2\pi(\Delta f) R_0}{c}, \end{aligned} \tag{7}$$

Solving Eq. (7) for the angle yields

$$\begin{aligned} \cos\theta_a &= \frac{f_0\cos\theta}{f} + \frac{\Delta f\cos\theta}{f} - \frac{\Delta f R_0}{fd} \\ \theta_a &= \arccos\left(\frac{f_0\cos\theta}{f} + \frac{\Delta f\cos\theta}{f} - \frac{\Delta f R_0}{fd} \right). \end{aligned} \tag{8}$$

It is worth remarking that a progressive phase shift of $\Delta\psi$ across the elements must be applied for scanning. In addition to this, a scan angle θ_0 must be defined to steer the main beam to the desired direction. Equation 7 defines the amount of phase shift for FDA, and the array factor can be calculated as below.

Taking the first element as the reference, the steering vector can be expressed as

$$\mathbf{a}(\theta, R) = \left[1 \quad e^{-j\left(\frac{2\pi f_0 d\cos\theta}{c} + \frac{2\pi(\Delta f) d\cos\theta}{c} - \frac{2\pi(\Delta f) R}{c} \right)} \cdots \right.$$
$$\left. e^{-j\left(\frac{2\pi f_0 (N-1) d\cos\theta}{c} + \frac{2\pi (N-1)^2 (\Delta f) d\cos\theta}{c} - \frac{2\pi (N-1)(\Delta f) R}{c} \right)} \right]^T, \tag{9}$$

where the superscript $(.)^T$ denotes the transpose operation.

Throughout this paper, we assume a narrowband system where the propagation delays manifest as phase shifts to the transmitted signals. For uniform beamforming weighting, the FDA array factor $AF(\theta, R)$ can be written by

$$AF(\theta,R) = \sum_{n=1}^{N-1} exp\{-j\gamma_0(f_0(n-1)d\cos\theta - (n-1)(\Delta f)R)\}, \tag{10}$$

$$AF(\theta,R) \approx \frac{exp\left\{jN\gamma_0\left(f_0 d\cos\theta - (\Delta f)R\right)\right\}}{exp\left\{j\gamma_0\left(f_0 d\cos\theta - (\Delta f)R\right)\right\}} \times \frac{\cos\left\{N\gamma_0\left(f_0 d\cos\theta - (\Delta f)R\right)\right\}}{\cos\left\{\gamma_0\left(f_0 d\cos\theta - (\Delta f)R\right)\right\}}, \tag{11}$$

where $\gamma_0 = 2\pi/c$. Herein, we assume that, $f_0 \gg \Delta f$ and $R \gg (N-1)d\cos\theta$.

The difference in the transmitted beampatterns of the conventional PAR and FDA radar is shown in Fig. 2, where 10 element uniform linear FDA with inter-element spacing denoted $d = \lambda/2$, the carrier frequency $f_0 = 1$ GHz. $\Delta f = 0$ and 350 Hz.

Herein, we give a summary of the FDA characteristics:

1. If the frequency offset (Δf) is fixed, the beam direction will vary as a function of the range R as can be seen in Fig. 2b. Thus, it is a range-dependent beampattern.
2. If the range R is fixed, the beam direction will vary as a function of the frequency increment (Δf) . This indicates that the FDA is also a frequency-increment dependent beampattern.
3. If the frequency increment across the array is not applied (i.e., $\Delta f = 0$), the corresponding FDA radar is just a conventional PAR (Fig. 2a).
4. Frequency scanning and FDA have similarities in terms of frequency diversity; however, frequency scanned arrays use the frequency increment as a function of time for all elements, while frequency diverse arrays use the frequency increment at the discrete points of the aperture [21].

It can be clearly seen that from the aforementioned considerations, the transmitted beampattern of the traditional PAR is angle-dependent while that of the FDA radar is range-angle-dependent, and hence, the FDA provides better control over modulation and beam synthesis when compared to the conventional phased array. More precisely, PAR beam is fixed at one angle for all the ranges, and hence, there is no range information, whereas it is unfixed and changeable in FDA ranges.

Based on the aforementioned concepts, this flexible beam scan option can be quite helpful for multiple target detection and tracking with advanced signal processing techniques due to local maxima at different ranges. Furthermore, the FDA might be a perfect way for protecting the radar from the deception jamming, since different frequencies are employed in the transmitted signal, which are not accessible for conventional PAR. Thus, the DRFM repeated jammer work will sufferer remarkably in order to regenerate precisely the replica of these multiple frequencies.

Although, the FDA radar gives more degrees of freedom and capabilities in range and angle to design and control the antenna beampattern and also enhances the overall performance and efficiency that might afford many novel potential applications. Nevertheless, such enhancements do not come for free. A major difficulty is the system and

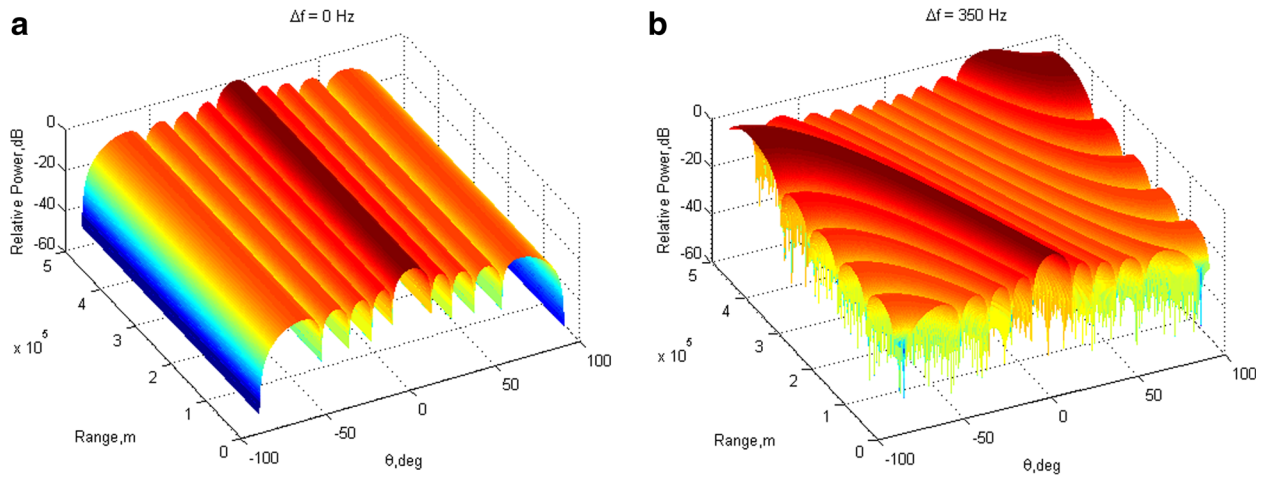

Fig. 2 Transmit beampattern comparisons between FDA and phased array. **a** Phased-array beampattern. **b** FDA beampattern

computational complexity. In addition to that, the range ambiguities still remain a great challenge and also the range and angle of the true target cannot be exclusively estimated from the FDA radar beamforming output peak due to the range-angle coupling response.

Several researches have been carried on FDA radar to alleviate its difficulties. The time and angle periodicity of FDA beampattern was analyzed in [27]. A linear FDA was proposed in [28] for forward-looking radar ground moving target indication. The multipath characteristics of FDA radar over a ground plane were investigated and compared with phased array in [29]. The impacts of frequency increment errors in the FDA beam pattern have been addressed in [30].

Moreover, in [31] the nonuniform FDA acts as a transmitter and the uniform phased array as the receiver to achieve range-angle imaging of targets was proposed. A symmetrical FDA beampattern synthesis method using multi-carrier frequency increments and convex optimization in which dot-shaped transmit beampatterns will be achieved for decoupling the range-angle response was investigated in [32].

Although recently the FDA has drawn great interest in antenna and radar areas, and many works in the area of FDA have been presented and assessed, but little work about the ECCM in FDA radars can be found. Thus, further research work should be carried out, especially in the ECCM area, because radars without ECCM are regarded as worthless and powerless of deploying in the hazard zones.

It is worth noting that, subarray-based FDA was originally used for localizing the target in the range-angle domain by exploiting the transmit-receive beamforming output peak. Accordingly, this paper moves a further step towards the subarray FDA configuration for deception jamming suppression.

3 Subarray-based FDA radar signal model for interference and false targets suppression

Originally, subarrays were utilized in order to reduce the computational burden, as the number of arrays might decrease considerably, especially for an antenna which contains huge number of elements.

Generally speaking, the arrays can be divided into multiple subarrays, which can be disjoint or overlapped. The subarray division is a system design problem; the optimized result has to take into account a variety of aspects because the selection of subarray design has a strong impact on the performance. However, different capabilities may be mutually contradictory as it is hard to determine how many subarrays are required and what shape they must have. As a result, the design of subarray partitioning is a complex dilemma both in theory and practice.

For FDA radar, the subarray partitioning is developed to decouple the range and angle response in the transmit beampattern towards better localization performance. Optimal design of FDA subarrays via Cramer-Rao lower bound (CRLB) minimization [20, 33] confirmed that two subarrays are the optimum choice in selecting the number of subarrays. Furthermore, the frequency offset Δf should be dissimilar and with opposite signs; that is, one is positive and the other is negative for each subarray to get lower angle CRLB . Nevertheless, for higher resolution Δf needs to be a higher value.

3.1 Subarray-based FDA signal model

Accordingly, the elements in Fig. 1 can be divided into two disjoint subarrays, each subarray has L elements. The first subarray employs the frequency increment Δf_1, whereas the second subarray employs the frequency increment Δf_2.

Then the frequency increments can be represented by

$$f_{first} = f_c + l \cdot \Delta f_1 \qquad l = 0, 1, 2, \ldots, L-1 \tag{12}$$

$$f_{second} = f_c + l \cdot \Delta f_2 \quad l = 0, 1, 2, \ldots, L-1 \tag{13}$$

Therefore, the transmit steering vector, by taking the first element as the reference for the array, can then be represented by

$$\begin{aligned}\mathbf{a}(\theta, R) = \Big[1 \quad & e^{-jw_1} \quad e^{-j2w_1} \quad \ldots \quad e^{-j(L-1)w_1} \\ & 1 \cdot e^{-jw_c} \quad e^{-j(w_c+w_2)} \quad e^{-j(w_c+2w_2)} \quad \ldots \\ & e^{-j[w_c+(L-1)]w_2)}\Big]^T,\end{aligned} \tag{14}$$

where

$$w_1 = \frac{2\pi f_0 d \sin\theta}{c_0} - \frac{2\pi \Delta f_1 R}{c_0}, \tag{15}$$

$$w_2 = \frac{2\pi f_0 d \sin\theta}{c_0} - \frac{2\pi \Delta f_2 R}{c_0}, \tag{16}$$

$$w_c = \frac{2\pi L f_0 d \sin\theta}{c_0}, \tag{17}$$

if we denote $S(t)$ to be the baseband waveform transmitted by each element, which consists of two different subarrays. Then, the baseband equivalent model, in a complex-valued form, of the transmitted signals from the $2L$ transmit elements can be expressed as

$$\mathbf{a}^*(\theta_0, R_0) S(t), \tag{18}$$

where $(.)^*$ denotes the conjugate and $\mathbf{a}(\theta_0, R_0)$ denotes the $2L \times 1$ transmit steering vector including complex-valued

elements with unit amplitude and phase determined by the look angle θ_0 and range R_0. The signal observed at a specific location with angle (θ_0 and range R_0) in the far-field is a superposition of the delayed and attenuated description of the transmitted signals [34] and can be written as

$$\mathbf{a}^T(\theta_i, R_i)\mathbf{a}^*(\theta_0, R_0)S(t-\tau) \triangleq \beta_i S(t-\tau), \tag{19}$$

where τ is the signal propagation time delay, and β_i is a constant for the target. The first $\mathbf{a}(\theta_i, R_i)$ on the left side is a propagation vector due to the propagation effects, which gets the same form as the steering vector. Thus, the signal at the look angle θ_0 and range R_0 is given by

$$\mathbf{a}^T(\theta_0, R_0)\mathbf{a}^*(\theta_0, R_0)S(t-\tau) = 2LS(t-\tau) = NS(t-\tau), \tag{20}$$

where there is a directional gain of $N = 2L$ (the size of the total transmit aperture) at the observed direction. This is a well-known property of PAR.

In the case that the deception jamming has not been applied, there is a target located at angle θ_0 and range R_0. The baseband corresponding to the signals at the receive array can be illustrated as below

$$X(t) = \alpha_0\mathbf{a}(\theta_0, R_0)\mathbf{a}^T(\theta_0, R_0)\mathbf{a}^*(\theta_0, R_0)S(t-2\tau) + n(t), \tag{21}$$

where α_0 is the complex amplitude of the source, the first $\mathbf{a}(\theta, R)$ is the propagation vector due to the propagation delay from a source to the receive elements, and $n(t)$ is the additive white Gaussian noise vector. Consequently, after matched filtering, the baseband equivalent of the complex-valued signals at the receive array can be expressed as

$$y \triangleq \frac{\int_{T_p} X(t)S^*(t)dt}{\int_{T_p} |S(t)|^2 dt} = \beta_0 \cdot \mathbf{a}(\theta_0, R_0) + \mathbf{v}, \tag{22}$$

where T_p is the coherent processing interval (CPI). CPI is a statistical measure of the time duration over which the received signal pulse responses are essentially invariant [10]. β_0 is a constant for a given target, and $\mathbf{v}$ is a complex Gaussian noise vector with zero mean and covariance σ_n^2. The target parameters can be estimated by the following optimization equation:

$$(\hat{\theta}, \hat{R}) = arg \quad max_{\theta,R}|w^H(\theta, R)y|^2, \tag{23}$$

where $(\cdot)^H$ is the conjugate transpose, and $\mathbf{w}(\theta, R)$ can be chosen as the non-windowed weight vector described as

$$\mathbf{w}(\theta, R) = \mathbf{a}(\theta, R). \tag{24}$$

3.2 Principle of interference and deceptive jamming suppression

Radar signal processing seeks for an optimum processing method in order to acquire target information. In the instance that there is no jammer or multiple interference source that tries to mislead the radar, the true targets can be well detected. On the contrary, when the radar system is jammed, target signals are often superimposed with jamming signals making it difficult to distinguish true and false targets, and thus, erroneous information can occur. For that reason, in order to accurately detect the desired target signals, jamming signals must be separated from target signals.

In this subsection, we discuss the characteristic of the interference and jammings. In the sequel, we propose a subarray FDA approach to detect the true target in interference and deceptive ECM scenarios.

Assuming that a target is located at (θ_0, R_0) and multiple interference sources are at (θ_i, R_i). Besides, a repeated jammer generates many false targets to deceive the radar system, and the baseband equivalent of the signals at the receive array can be expressed as Eq. (21) in [35] by

$$\begin{aligned} X(t) = {} & \alpha_0\beta_0\mathbf{a}(\theta_0, R_0)S(t-2\tau) + \sum_{i=1}^{I}\alpha_i\beta_i\mathbf{a}_r(\theta_i, R_i)S(t-2\tau) \\ & + \sum_{k=1}^{K}\alpha_k\beta_k\mathbf{a}_r(\theta_k, R_k)S\left((t-t_k) - 2(\tau-\tau_k)\right) + n(t), \end{aligned} \tag{25}$$

where α_i and α_k denote, respectively, the complex amplitudes of the ith interference source and the kth false target, (θ_k, R_k) are the range and angle parameters of the kth false target, and t_k and τ_k are due to the observing time and the time delay of the jammer, respectively. Note that the correlated clutter can be consider as the interferences. By matched-filtering the received signal to the transmitted signal $S(t)$, we can get

$$\begin{aligned} y & \triangleq \frac{\int_{T_p} X(t)S^*(t)dt}{\int_{T_p} |S(t)|^2 dt} \\ & \triangleq \alpha_0\mathbf{u}(\theta_0, R_0) + \sum_{i=1}^{I}\alpha_i\mathbf{u}(\theta_i, R_i) + \sum_{k=1}^{K}\alpha_k\mathbf{u}(\theta_k, R_k) + \mathbf{v}, \end{aligned} \tag{26}$$

where the interference virtual steering vector

$$\mathbf{u}(\theta_i, R_i) \triangleq \beta_i \cdot \mathbf{a}(\theta_i, R_i), \tag{27}$$

the deceptive jamming virtual steering vector can be written as

$$\mathbf{u}(\theta_k, R_k) \triangleq \beta_k \cdot \mathbf{a}(\theta_k, R_k - R), \tag{28}$$

where the $(\theta_k, R_k - R)$ are due to frequency offset.

Therefore, the received signals consist of the target, multiple interference , deception jamming, and noise as below

$$X(t) = X_{tar}(t) + X_{int} + X_{dec}(t) + X_n(t). \tag{29}$$

Herein, we can express the covariance matrix as

$$C_y \triangleq E\left\{yy^H\right\} = C_{tar} + C_{int} + C_{dec} + C_n, \tag{30}$$

where $C_{tar} = E\{x_{tar}(t)x_{tar}(t)^H\}$, $C_{int} = E\{x_{int}(t)x_{int}(t)^H\}$, $C_{dec} = E\{x_{dec}(t)x_{dec}(t)^H\}$ and $C_n = E\{x_n(t)x_n(t)^H\}$ are the target covariance matrix, interference covariance matrix, deceptive jamming covariance matrix, and noise covariance matrix, respectively.

Note that $C_n = {\sigma_n}^2 I$. Herein, the $E\{\cdot\}$ denotes the expectation operator and I is an identify matrix. The interference covariance matrix can be represented by

$$C_{int} = \sum_{i=1}^{I} \sigma_i^2 \mathbf{u}(\theta_i, R_i)\mathbf{u}^H(\theta_i, R_i). \tag{31}$$

The deceptive jamming covariance matrix can be denoted by

$$C_{dec} = \sum_{k=1}^{K} \sigma_k^2 \mathbf{u}(\theta_k, R_k)\mathbf{u}^H(\theta_k, R_k). \tag{32}$$

Using Eqs. (14) and (26), we can estimate the true target ranges and angles by optimally designing the transmit beamspace matrix $\mathbf{a}(\theta_0, R_0)$.

Several signal-processing-based techniques for rejection of unwanted signals have been proposed in [36–40]. In addition, the beamspace design for PAR is examined in [41]. In this paper, we make use of the transmit beamspace of FDA radar design that was investigated in [35]. Since the amplitude and spatial distribution of the FDA range-angle beampattern can be controlled by the frequency increments and number of the elements in the array, the transmitted energy in a desired range-angle region can carefully focus by designing the beamspace matrix and thus the two-dimensional positions can be unambiguously estimated. Therefore, the steps of designing the transmit beamspace matrix included [35]: (1) formulating the transmit beamspace design as an optimization problem, (2) designing the quiescent response vector, and (3) solving the second-order cone (SOC) program to get the optimized transmit beamspace.

Therefore, the following aspects are taken into consideration:

- Compensating the frequency increments allows us to process the received signals at subarray level perfectly since it allows the time associated with the observed point range gate for the true target to be identical for all elements.
- The range-angle-dependent beam provides a potential to suppress range-dependent interferences and noise. Since basic FDA radar can suppress range-dependent interferences, the subarray-based FDA radar has better robustness against interference.
- In spite of the fact that the repeated jammer can proficiently regenerate the false targets with different carrier frequencies. However, it will also experience some confusion due to the multiple frequencies encountered.
- All the false targets are produced by the similar deception signals, and as a result of which, their appearing time sequence, the intervals, and the amplitude fluctuation are all the same in every element, since they share the same transmit and receive spatial frequencies.
- Moreover, contrary to the false targets, the true targets have their own velocity, and therefore, by combining the information from all the elements at subarray level, the targets appear as identical replica at subarray outputs.
- On the other hand, all the false targets generated by the repeated jammer will not share the same frequency offsets (Δf) and hence will not be probably identical, especially in combining the subarry outputs.

After the transmit beamspace design procedure, we can then construct MUSIC based for estimating the range and angle of the target.

Consequently, the eigendecomposition of array covariance matrix in Eq. (30) can then be rewritten as

$$C_y \triangleq \mathbf{E}_{tar}\mathbf{\Lambda}_{tar}\mathbf{E}_{tar}^H + \mathbf{E}_{int}\mathbf{\Lambda}_{int}\mathbf{E}_{int}^H + \mathbf{E}_{dec}\mathbf{\Lambda}_{dec}\mathbf{E}_{dec}^H + \mathbf{E}_n\mathbf{\Lambda}_n\mathbf{E}_n^H, \tag{33}$$

where the diagonal matrix $\mathbf{\Lambda}_{tar}$ contains the largest eigenvalue and the columns of $_{tar}$ are the corresponding eigenvectors, whereas the diagonal matrix $\mathbf{\Lambda}_{int}$, $\mathbf{\Lambda}_{dec}$, and $\mathbf{\Lambda}_n$ contain the remaining unwanted eigenvalues and the

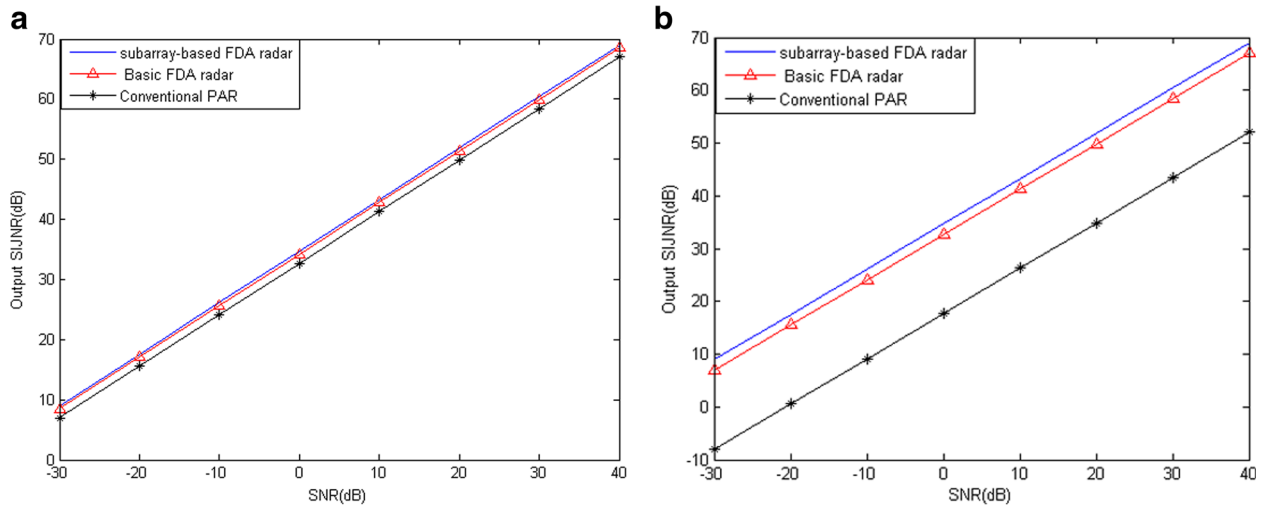

Fig. 3 Output SIJNR versus SNR performance. **a** In the absence of ECM signals. **b** In the presence of ECM signals

columns of $\mathbf{E}_{int}$, $\mathbf{E}_{dec}$, and $\mathbf{E}_n$ are the corresponding eigenvectors.

The transmit beamspace-based MUSIC cost function is [42].

$$f(\theta,R)=\frac{\mathbf{u}^H(\theta,R)\mathbf{u}(\theta,R)}{\mathbf{u}^H(\theta,R)\mathbf{P}\mathbf{u}(\theta,R)} \tag{34}$$

$$\mathbf{P}=\mathbf{E}_{int}\mathbf{E}_{int}^H+\mathbf{E}_{dec}\mathbf{E}_{dec}^H+\mathbf{E}_n\mathbf{E}_n^H \tag{35}$$

The range and angle estimates are given by the magnitude peaks of Eq. (36) using the weight vector $\mathbf{w}$ described in Eq. (24) and hence can be written as

$$(\tilde{\theta},\tilde{R})=arg \quad max_{\theta,R}|f(\theta,R)|. \tag{36}$$

The conventional nonadaptive beamforming is used here in the sense that it provides the highest possible output signal-to-noise ratio (SNR) and the signal-to-interference-plus-jamming-plus-noise ratio (SIJNR) in the subarray-based FDA. Consequently, we use the conventional non adaptive beamforming at both the transmitted and received arrays of the FDA radar system and output SIJNR performance.

The output SIJNR of the FDA radar can be evaluated by

$$SIJNR\triangleq\frac{\sigma_{tar}^2|\mathbf{w}^H\mathbf{u}(\theta_0,R_0)|^2}{\mathbf{w}(C_{int}+C_{dec}+C_n)\mathbf{w}}, \tag{37}$$

where σ_{tar}^2 is the variance of the desired target signal. Substituting C_{int}, C_{dec}, and C_n to Eq. (37) yields

It is noticed that like PAR, the subarray-based FDA radar has coherent transmit processing gain; but, the FDA directional gain depends on both the range and angle parameters, while PAR directional gain depends just on the angle parameter. This feature coupled with frequency offset compensation for subarray output yields achievable prospective for suppression of the interference , false targets and noise. Thus, the parameter vector estimated by applying the weight vector to the matched filtering the received signal in all subarrays, and hence, the true target location can be discriminated from other unwanted signals in the peak of the beamforming output.

The FDA radar signal detection problem can be modeled as Neyman-Pearson detection, by utilizing the binary hypothesis test that was investigated in [43].

4 Simulation results and discussion

In this Section, simulations are conducted to assess the false target suppression performance of the proposed method. In the simulation scenario, we suppose a ULA FDA radar with carrier frequency $f_0 = 10$ GHz and frequency increments $\Delta f_1 = 30$ kHz and $\Delta f_2 = 10$ kHz. In addition, 20 elements are utilized for transmitting and 20 elements are exploited for receiving. The distance between adjacent elements is $\lambda_0/2$ (λ is wavelength) to avoid the aliasing. In this scenario, one target with power fixed to 10 dB reflects a plane-wave that impinges on the all arrays from the direction angle $\theta_0 = 0°$ and range R_0

$$SIJNR=\frac{\sigma_{tar}^2N^2}{\sum_{i=1}^{I}\sigma_i^2|\mathbf{a}^H(\theta_0,R_0)\mathbf{a}(\theta_i,R_i)||\mathbf{a}^H(\theta_0,R_0)\mathbf{a}(\theta_i,R_i)|+\sum_{k=1}^{K}\sigma_k^2|\mathbf{a}^H(\theta_0,R_0)\mathbf{a}(\theta_k,R_k)||\mathbf{a}^H(\theta_0,R_0)\mathbf{a}(\theta_k,R_k)|+\sigma_n^2N}. \tag{38}$$

= 20 km. A repeated jammer re-reflects this target signal to all arrays, and therefore creates false targets (two false targets with power 20 dB are assumed) in direction angles $\theta_1 = 20°$ and $\theta_2 = 40°$, with mimicked ranges $R_1 = 50$ km and $R_2 = 30$ km, respectively. Further suppose there are one interference located at the direction angle $\theta_i = 10°$ and range $R_i = 10$ km. The interference power is fixed to 15 dB.

Firstly, the SIJNR versus SNR is addressed in order to evaluate the subarray-based FDA radar performance. Also, we will compare subarray-based FDA radar to the FDA and PAR with the same array parameters. Figure 3 compares the SIJNR vs SNR.

As per the simulation results in Fig. 3a, the conventional PAR performed slightly less than FDA and subarray-based FDA radar when there was no effect of the ECM signals. Besides, the FDA has similar behavior as compared to the subarray-based FDA in the absence of ECM scenario. However, in the presence of the deceptive jamming and interference as shown in Fig. 3b, the PAR performance degraded dramatically. Also, subarray-based FDA outperformed the FDA radar. As a result, in the occurrence of the unwanted interference and deceptive jamming, the subarray-based FDA can discriminate the true target from the false ones at the output of the processor. Therefore, the proposed method can handle the deceptive jamming successfully.

Secondly, Fig. 4 assesses the detection and performance of the proposed method. Figure 4 shows the comparative detection probability (P_d) performance as a function of the SNR. The detection probability is defined as the probability of declaring a target to be present. Therefore, the detection probabilities of the PAR, FDA, and subarray-based FDA radar are plotted, in view of the scenarios with and without ECM. In Fig. 4, we have the same system parameters as in Fig. 3, but the false alarm probability P_{fa} is set to 10^{-6}. It can be noticed that all the comparative radars give a satisfactory estimation performance without deception jamming targets as shown in Fig. 4a. From a quantitative point of view in Fig. 4b, the detection probability of the PAR degrades considerably in scenarios with ECM. Moreover, FDA has a moderate P_d as compared to subarray-based FDA radar.

The numerical results reported in Fig. 4 are in agreement with the considerations above. It is seen that the best performance is still attained by the subarray-based FDA radar.

Moreover, it is worth pointing out that all of the aforementioned simulations are carried out by resorting to standard Monte Carlo counting techniques.

Finally, Fig. 5 highlights the beam pattern obtained by subarray-based FDA radar after compensating the frequency increments and combining the subarrays signals. The beam pattern in both angle and Doppler (space-time) domains is depicted. It is obviously seen that the target is well maintained and the jamming signals and the interference are effectively rejected.

5 Conclusions

The conflict between ECM and ECCM is a permanent combat. There is no jamming that cannot be suppressed, and no radar that cannot be jammed. In this paper, it has been shown that subarray-based FDA radar provides an alternative and flexible way for ECCM methods. Since it is difficult for basic FDA radar to directly estimate both the range and angle of a target from the beamformer output, thus we divided the FDA array into two subarrays, which occupy two different frequency increments. In doing so, the desired target is distinguished at subarray level in joint range-angle-Doppler domains, according to the fact that the jammer generated false targets with the same ranges at each subarray without reparations. The performance

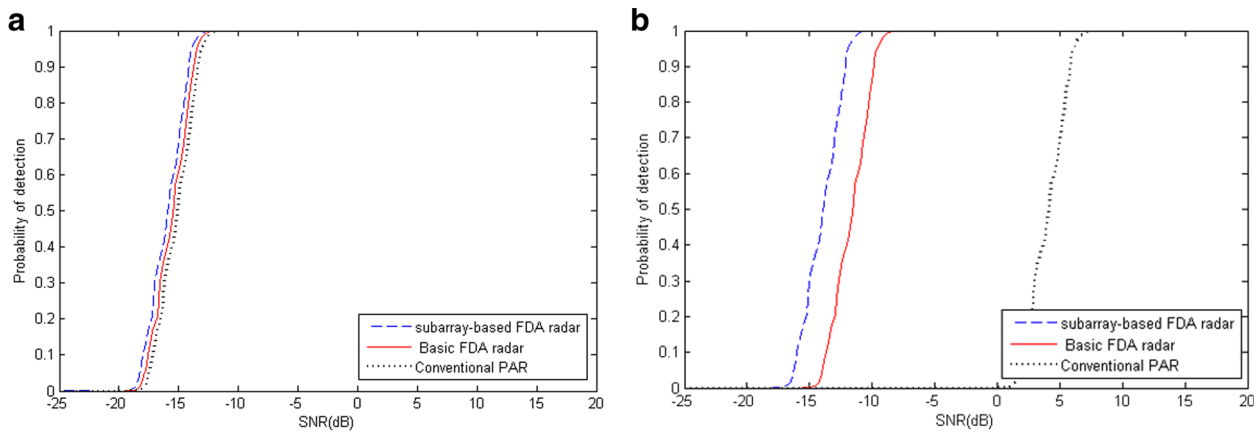

Fig. 4 Detection probability versus SNR performance. **a** In the absence of ECM signals. **b** In the presence of ECM signals

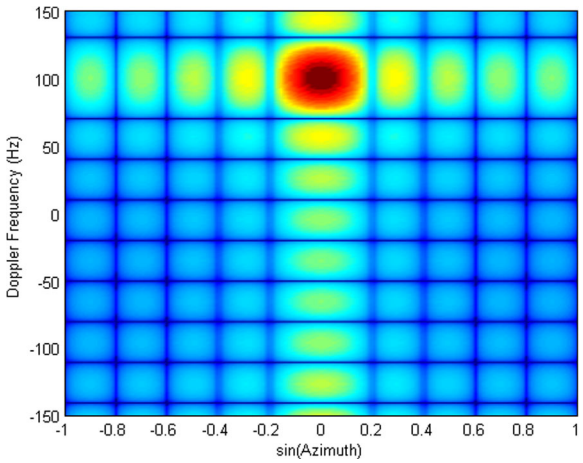

Fig. 5 The beam pattern obtained by subarray-based FDA radar

analysis showed that the proposed solutions are powerful in presence of ECM systems. Furthermore, the output SIJNR is remarkably enhanced.

It is needed to note that nonadaptive beamforming on the receiver is used in this paper. It can be expected that if adaptive beamformer is utilized on the receiver the jamming suppression performance might be further improved.

Finally, it is worth remarking that the FDA has attracted much attention in recent years; however, its application in electronic warfare has not been investigated and thus, further studies need to be carried out.

Acknowledgements
The authors express their gratitude to the editor and anonymous reviewers for their helpful comments and suggestions that improved this paper.

Competing interests
The authors declare that they have no competing interests.

Received: 6 July 2016 Accepted: 22 September 2016
Published online: 03 October 2016

References

1. V Gracheva, E Joachim, Multichannel analysis and suppression of sea clutter for airborne microwave radar systems. IEEE Trans. Geosci. Remote Sens. **54**(4), 2385–2399 (2016)
2. E Alaa, K Assaleh, H Mir, Space-time adaptive processing using pattern classification. IEEE Trans. Signal Process. **63**(3), 766–779 (2015)
3. S Pawan, R Muralidhar, Waveform design for radar STAP in signal dependent interference. IEEE Trans. Signal Process. **64**(1), 19–34 (2016)
4. C Diego, W Ingo, Joint Monostatic and Bistatic STAP for improved SAR-GMTI capabilities. IEEE Trans. Geosci. Remote Sens. **54**(3), 1834–1848 (2016)
5. Z Wang, W Yongliang, D Keqing, X Wenchong, Subspace-augmented clutter suppression technique for STAP Radar. IEEE Trans. Geosci. Remote Sens Lett. **13**(3), 462–466 (2016)
6. H Wang, G Liao, L Jun, W Guo, Robust waveform design for MIMO-STAP to improve the worst-case detection performance. EURASIP J. Adv. Signal Process. **2013**(52), 1–8 (2013)
7. S Roome, Digital radio frequency memory. IEE Electronics Commun. Eng. J. **2**(4), 147–153 (1990)
8. Y Hiong, H Gu, Y Zhang, T Bin, in *Proceedings of the International Conference on Advanced Computer Science and Electronics Information, Hangzhou, China*. An investigation of range-velocity deception jamming modeling, (2013), pp. 59–63
9. J Akhtar, Orthogonal block coded ECCM schemes against repeat radar jammers. IEEE Trans. Aerosp. Electron. Syst. **45**(3), 1218–1226 (2009)
10. A Ahmed, Y Zhao, R Mohammed, T Bin, An improved radar eccm method based on orthogonal pulse block and parallel matching filter. J. Commun. **10**(8), 610–614 (2015)
11. J Zhang, D Zhu, G Zhang, New antivelocity deception jamming technique using pulses with adaptive initial phases. IEEE Trans. Aerosp.Electron. Syst. **49**(2), 1290–1300 (2013)
12. B Rao, S Xiao, X Wang, T Wang, Maximum likelihood approach to the estimation and discrimination of exoatmospheric active phantom tracks using motion features. IEEE Trans. Aerosp. Electron. Syst. **48**(1), 794–819 (2012)
13. A Coluccia, G Ricci, ABORT-Like detection strategies to combat possible deceptive ECM signals in a network of radars. IEEE Trans. Signal Process. **63**(11), 2904–2914 (2015)
14. F Bandiera, A Farina, D Orlando, G Ricci, Detection algorithms to discriminate between radar targets and ECM signals. IEEE Trans. Signal Process. **58**(12), 5489–5993 (2010)
15. M Greco, F Gini, A Farina, Radar detection and classification of jamming signals belonging to a cone class. IEEE Trans. Signal Process. **56**(5), 1984–1993 (2008)
16. J Xu, S Zhu, G Liao, Space-time-range adaptive processing for airborne radar systems. IEEE Sensors J. **58**(12), 1602–1610 (2015)
17. J Xu, G Liao, S Zhu, H Cheung So, Deceptive jamming suppression with frequency diverse MIMO radar. Signal Process. **113**, 9–17 (2015)
18. A Hassanien, SA Vorobyov, Why the phased-mimo radar outperforms the phased-array and mimo radars. 18th European Signal Processing Conference *(EUSIPCO-2010) EURASIP*, August 23-27 Aalborg, Denmark, 2010, (2010). ISSN 2076–1465
19. H Hu, Aspects of the subarrayed array processing for the phased array radar. Int. J. Antennas Propag. **2015**(4), 1–21 (2015)
20. W-Q Wang, Subarray-based frequency diverse array radar for target range-angle estimation. IEEE Trans. Aerosp. Electron. Syst. **50**(4), 3057–3067 (2014)
21. W-Q Wang, Frequency diverse array antenna: new opportunities. IEEE Antennas Propag. Mag. **57**(2), 145–152 (2015)
22. W-Q Wang, Phased-MIMO radar with frequency diversity for range-dependent beamforming. IEEE Sensors J. **13**(4), 1320–1328 (2013)
23. P Antonik, MC Wicks, HD Griffiths, CJ Baker, in *Proc. IEEE Radar Conf.* Frequency diverse array radars (IEEE, Italy, 2006), pp. 215–217
24. P Antonik, MC Wicks, HD Griffiths, CJ Baker, in *Proc. IEEE Radar Conf.* Multi-mission multi-mode waveform diversity (IEEE, Italy, 2006), pp. 580–582
25. P Antonik, MC Wicks, Method and apparatus for simultaneous synthetic aperture radar and moving target indication. U.S. Patent No. 7,646,326. 12 Jan. 2010
26. P Antonik, MC Wicks, HD Griffiths, CJ Baker, in *Proc. Int. Waveform Diversity Des. Conf.* Range dependent beamforming using element level waveform diversity (IEEE, Las Vegas, 2006), pp. 1–4
27. M Secmen, S Demir, A Hizal, T Eker, in *Proceedings of the IEEE Radar Conference*. Frequency diverse array antenna with periodic time modulated pattern in range and angle (IEEE, Boston, 2007), pp. 427–430
28. P Baizert, TB Hale, MA Temple, MC Wicks, Forward-looking radar GMTI benefits using a linear frequency diverse array. Electron. Lett. **42**(22), 1311–1312 (2006)
29. C Cetintepe, S Demir, Multipath characteristics of frequency diverse arrays over a ground plane. IEEE Trans. Antennas Propag. **62**(7), 3567–3574 (2014)
30. K Gao, C Hui, H Shao, J Cai, W-Q Wang, Impacts of frequency increment errors on frequency diverse array beampattern. EURASIP J. Adv. Signal Process. **2015**(1), 1–12 (2015)
31. W Wen-Qin, HC So, H Shao, Nonuniform frequency diverse array for range-angle imaging of targets. IEEE Sensors J. **14**(8), 2469–2476 (2014)
32. H Shao, J Dai, J Xiong, H Chen, W Wen-Qin, Dot-shaped range-angle Beampattern synthesis for frequency diverse array. IEEE Antenna Wireless Propag. Lett. **PP**(99), 1–1 (2016). doi:10.1109/LAWP.2016.2527818

33. W Yongbing, W Wen-Qin, H Shao, J Xiong, H Chen, Optimal frequency diverse subarray design with Cramér-Rao lower bound minimization. IEEE Antenna Wireless Propag. Lett. **14**, 1188–1191 (2015)
34. MG Sullivan, *Practical Array Processing*. (McGraw Hill, New York, 2009)
35. W-Q Wang, HC So, Transmit subaperturing for range and angle estimation in frequency diverse array radar. IEEE Trans. Signal Process. **62**(8), 2000–2011 (2014)
36. F Bandiera, A De Maio, G Ricci, Adaptive CFAR radar detection with conic rejection. IEEE Trans. Signal Process. **55**(6), 2533–2541 (2007)
37. NB Pulsone, CM Rader, Adaptive beamformer orthogonal rejection rest. IEEE Trans. Signal Process. **49**(3), 521–529 (2001)
38. F Bandiera, D Orlando, G Ricci, *Advanced radar detection schemes under mismatched signal models*. (Morgan and Claypool Publishers, New York, 2009)
39. F Bandiera, O Besson, G Ricci, An ABORT-like detector with improved mismatched signals rejection capabilities. IEEE Trans. Signal Process. **56**(1), 14–25 (2008)
40. F Bandiera, D Orlando, G Ricci, One-stage tunable receivers. IEEE Trans. Signal Process. **57**(8), 3264–3273 (2009)
41. A Hassanien, SA Elkader, AB Gershman, KM Wong, Convex optimization based beam-space preprocessing with improved robustness against out-of-sector sources. IEEE Trans. Signal Process. **54**(5), 1587–1595 (2006)
42. XL Xu, KM Buckley, An analysis of beam-space source localization. IEEE Trans. Signal Process. **41**(1), 501–504 (1993)
43. W-Q Wang, HC So, Range-angle localization of targets by a double-pulse frequency diverse array radar. IEEE J. Selected Topics Signal Processing. **8**(1), 106–114 (2014)